Hydrogen Response in Liquid Propylene Polymerization

Al-haj Ali, M.; Betlem, B.; Roffel, B.; Weickert, G.

Published in:
AIChE Journal

DOI:
10.1002/aic.10783

Hydrogen Response in Liquid Propylene Polymerization: Towards a Generalized Model

M. Al-haj Ali, B. Betlem, B. Roffel, and G. Weickert
University of Twente, Enschede, The Netherlands

DOI 10.1002/aic.10783
Published online February 6, 2006 in Wiley InterScience (www.interscience.wiley.com).

Liquid propylene batch experiments in the absence of a gas phase have been carried out using a highly-active $MgCl_2/TiCl_4$/phthalate/silane/AlR_3 catalyst at varying temperatures (60-80°C) and molar hydrogen-monomer ratios of 0-10 mmol/mol. With increasing hydrogen concentration the

- *polymerization rate increases rapidly, reaching a constant value at concentrations above 1.4 mmol/mol;*
- *pseudo-first-order catalyst deactivation constant increases;*
- *molecular weight decreases;*
- *polydispersity decreases slightly;*

*but average molecular weight and polydispersity increase with increasing temperature. Polymerization rate, deactivation constant, and average molecular weight can be modeled based on a consistent dormant site mechanism assuming an (averaged) quasi-single-site model.**AIChE J,* 52: 1866–1876, 2006
Keywords: liquid phase propylene polymerization, polymerization kinetics, dormant-site theory, molecular weight distribution, catalyst decay, hydrogen response

Introduction

Only a very few experimental studies have been carried out so far to investigate the effect of hydrogen during liquid propylene polymerization; most studies were performed in either a gaseous monomer or slurry,[1-15] but gas phase and slurry phase results cannot easily be compared and heat and sorption effects and mass transfer limitations may play a role.[16]

Polymerization rate

Some researchers measured polymerization yields in liquid propylene,[17,18] but much more kinetic information can be extracted from polymerization rate profiles. The first article reporting rate profiles in catalytic liquid propylene polymerization was published by Samson et al.,[4] and a number of other authors investigated the hydrogen effect on kinetics (see Pater et al.[2] and Shimizu et al.[3]). The reactor used was always partially-filled, and polymerizations were carried out in the presence of a gas phase, which can introduce mass transfer problems, see ref. [19].

Molecular weight

In 1959, Natta et al.[20] studied the effect of hydrogen on the molecular weight of the produced polymer for a $TiCl_3$/$Al(C_2H_5)_3$ catalyst. Their results showed that the number average molecular weight of both polyethylene and polypropylene could be described by the square root of the hydrogen partial pressure in the reactor, Eq. 1:

$$M_n = \frac{1}{K_1 + K_2 \cdot \sqrt{P_{H_2}}} \tag{1}$$

The authors concluded that hydrogen is adsorbed on the catalyst surface where it dissociates (Eq. 2) before it reacts with the growing polymer.

$$H_2 \rightleftarrows H^{(+)} + H^{(-)} \tag{2}$$

Correspondence concerning this article should be addressed to G. Weickert at g.weickert@tnw.utwente.nl.

Table 1. Most Important Publications on the Influence of Hydrogen in Catalytic Olefin Polymerization

Author	System Studied	Findings
Keii et al.[22]	TiCl4/$MgCl_2$/$C_6H_5COOC_2H_5$/$Al(C_2H_5)_3$ Gas phase propylene	Agreed with Eq. 1
Soga & Siono[23]	$TiCl_4$/$MgCl_2$/$Al(C_2H_5)_3$/ethyl benzoate 40°C; slurry propylene	Atactic PP is formed by atomic hydrogen transfer; isotactic PP results from molecular H_2 transfer
Guastalla & Gianinni[14]	$TiCl_4$/$MgCl_2$/$Al(C_2H_5)_3$ slurry propylene and ethylene	Mw of different polymer fractions is reduced following Eq. 1
Ross[21]	$TiCl_3 \cdot$ AA/DEAC Gas phase propylene	Eq. 1 fits best
Hindryckx et al.[49]	$MgCl_2$-based $TiCl_3$ Slurry, ethylene	Eq. 1
Busico et al.[26]	Wide range of hydrogen partial pressure studied	Eq. 1
Meier et al.[42]	Metallocene Gas phase, propylene $0 \leq C_{H_2}/C_{propylene} \leq 0.0016$	Inverse Mw depends linearly on hydrogen (linearization possible in a narrow H_2 range)
Kissin et al.[24]	$TiCl_4$/dibutylphthalate/$MgCl_2$ $0 \leq C_{H_2}/C_{propylene} \leq 0.08$	Mw-H_2: linear at low hydrogen, but constant at high hydrogen; polymer H_2 complex formed

Some of the most important findings are summarized in Table 1. All these studies were carried out either in a gas-phase[21,22] or slurry.[23-26] While most of them support the Natta model (Eq. 1), some differ.

Catalyst deactivation

One of the most widely supported hypotheses for catalyst activity decay is the over-reduction of the active centers, Ti^{3+}, into inactive form, Ti^{2+}, by the cocatalyst.[12,13,15,27-29] Keii et al.[15] examined the effect of cocatalyst addition, Triethylaluminum (TEA), whereas Busico et al.[28] showed a rapid second-order decay of the polymerization rate explained by clustered low-active Ti^{+2} species. However, Albizzati et al.[30] studied [η^6-areneTiAl_2Cl_8] and found that catalysts containing Ti^{+2} are active in propylene polymerization and the catalyst decay cannot be explained by the reduction of active trivalent Ti. Shimizu et al.[3] showed that higher TEA concentrations can lead to lower decay rates.

Many authors proposed different chemically-based mechanisms. Chien and Nozaki[31] explained the polymerization rate decay by the reaction of *adjacent* pairs of Ti^{+3} with monomer. Based on their observations, Guyot et al.[32] suggested that catalyst deactivation results from the formation of inactive Π-allyl species with saturation of the polymer chain end.

Different authors have already claimed that a monomer mass transfer limitation is not the cause of the rate decay[12,15,28,29]; however, others still support this hypothesis.[5] Also, Han-Adebekun et al.[6] showed that the effectiveness factor for highly crystalline propylene is smaller than 1.0.

In this article:

(1) Liquid propylene polymerization with a highly active catalyst in an over-pressured fully filled batch reactor is investigated. At these conditions, all the hydrogen is dissolved in liquid propylene and gas-liquid mass transfer is excluded.

(2) The influence of polymerization temperature and hydrogen concentration on polymerization kinetics and molecular weight is studied in a wide range of hydrogen concentrations.

(3) Models are presented and compared to quantify the effect of temperature and hydrogen concentration on the initial polymerization rate, the catalyst deactivation, and the polymer molecular weight.

Experimental

Chemicals

Propylene used in the experiments was "polymerization grade" and obtained from Indugas. The purity was more than 99.5%, with propane as a main impurity. Hydrogen used had a purity higher than 99.999%; it was further purified by passing it over a reduced BTS copper catalyst, obtained from BASF, and subsequently passing it through three different beds of molecular sieves, with pore sizes of 13, 4, and 3 Å, respectively. Propylene was purified in the same way; additionally, it was passed over a bed of oxidized BTS catalyst to remove CO. $TiCl_4$ supported on $MgCl_2$ with phthalate as internal donor and an external silane donor was used as a catalyst, with TEA as a cocatalyst and scavenger.

Reactor system

A 5-liter stainless steel jacketed batch reactor (Büchi BEP 280) with a separately heated cover plate was used; it is described elsewhere.[2-4] For intensive mixing, the reactor was equipped with a turbine stirrer operated at 2000 rpm. The pneumatic injection system allows the introduction of liquids and slurries into the reactor, even at high reactor pressures. The cooling medium temperature is kept constant within $\pm$ 0.01 K during isoperibolic experiments.

Experimental procedure

The reactor was flushed with nitrogen gas five times at 90°C and was purged with propylene gas at the beginning of the experiment, then filled with liquid propylene and heated up to the reaction temperature. When the temperature reached the setpoint, hydrogen was injected. The reactor temperature and pressure were monitored as a function of time. As soon as both became stable for an interval of 3 minutes, the reaction was started by injecting the prepared catalyst into the reactor.

The experiments were executed under isoperibolic conditions. Thus, just after the catalyst injection, the temperature control system becomes active in trying to keep the jacket temperature constant; the reaction temperature increases slightly, reaching a quasi-steady-state after about 1.5 minutes in the case of using a fully pre-activated catalyst. The heat of

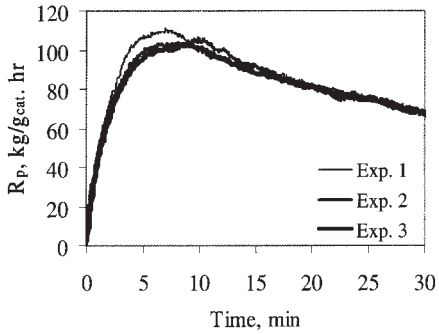

Figure 1. Polymerization rate-time profiles of repeated standard experiments.

polymerization is measured under quasi-steady state conditions. Data were collected every three seconds. The polymerization reaction was finally terminated by rapidly flushing the unreacted propylene. After each experiment, the resulting polymer was dried under vacuum at 50°C for 4 hours. The molecular weight distribution was measured by Gel Permeation Chromatography (GPC) employing a Waters Alliance GPCV 2000 apparatus with TSK columns at 155°C using 1,2,4-trichlorobenzene as a solvent. The GPC is calibrated with the narrow molecular weight distribution polystyrene standard as a reference. Average molecular weights above 1 million grams per mol have been measured using calibrated intrinsic viscosities.

Results and Discussion

Reproducibility

The reproducibility of the experiments has been tested by repeating a standard experiment at 70°C and 43 bar with 150 mg hydrogen at fixed concentrations of the catalyst, cocatalyst, and external donor. Figure 1 shows the reaction rate profiles for three standard experiments. The increase in polymerization rate during the first 1.5 minutes is not real, but caused by the (incorrect) application of the quasi-steady-state assumption for the heat balance during the initial phase. We will ignore this effect for the moment, but will come back to this point later. Obviously, the absence of a gas phase, i.e., absence of any mass transfer between gas and liquid phase, increases the accuracy of such rate profile measurements.

Isoperibolic initial polymerization rate

Reaction calorimeters can be classified according to their way of controlling the reaction temperature into the following categories: (i) isothermal, (ii) adiabatic, and (iii) isoperibolic. Using an isoperibolic calorimeter, the jacket temperature is kept constant, whereas the reaction temperature slightly increases during the exothermic reaction. However, the polymerization temperature can be kept within a small range producing "quasi-isothermal" data. The isoperibolic calorimeter has many advantages compared to the other calorimetric methods as discussed in [33,34]

The region where the rate of polymerization reaches the quasi-steady-state near the maximum, II in Figure 2, is a significant kinetic fingerprint in calorimetric observations of catalytic polymerizations,[35,36] but the question is how to estimate the "true" initial polymerization rate. We estimated two different initial polymerization rates: R_{po}, by extrapolating the reaction rate curve to time zero; and $R_{po,ATR}$, which can be calculated from the initial adiabatic temperature rise assuming that the heat produced mainly heats up propylene during the first seconds, see Table 2. For almost all runs, R_{po} is higher than $R_{po,ATR}$, but because of the uncertainties of all differential ("slope") methods combined with the assumption of adiabatic conditions and taking into account the data acquisition frequency of "only" 0.3 s^{-1}, we interpret these findings in terms of a fully pre-activated catalyst, i.e., the extrapolated value R_{po} can be used as the "true" initial polymerization rate.

It is relatively easy to check this "extrapolation hypothesis" by varying the reaction time. If the yield, Y, of such experiments can be estimated from the area underneath the extrapolated (isoperibolic) temperature difference, ΔT (time curve), but for different reaction times, then this hypothesis is true. First, this area is estimated for two ΔT profiles:

(1) A_1 from ΔT recorded directly starting at zero rate, Figure 3a; and

(2) A_2 from ΔT by extrapolating the curve to time zero, Figure 3b.

Clearly, it holds always that $A_2 > A_1$. The results are shown in Table 2. For example, for experiment 7 we estimate $Y/A_1 = 2.2$ and $Y/A_2 = 2.06$, respectively. These results are not significantly different, because of the relatively small contribution of the initial period. However, the situation changes—as expected—for a short-time experiment, carried out under similar conditions, but stopped after 7.5 minutes, experiment 14; see Table 2 and Figure 4, with $Y/A_1 = 2.95$ and $Y/A_2 = 1.95$. The latter value comes close to the value of the long-lasting experiment 7, whereas the model based on A_1 fails, with 30% deviation. This has two major consequences:

(1) The polymerization rate profile should be corrected by extrapolating the measured profile to time zero. The yield measured is represented by the area underneath this corrected rate-time curve.

(2) Y/A_2 should be calculated for a given reactor system. By means of this ratio, one can estimate yield and polymerization rate on-line directly from the temperature difference during an isoperibolic experiment.

The kinetic behavior of different catalyst systems can be very different, but the method used above can be applied to clarify this point.

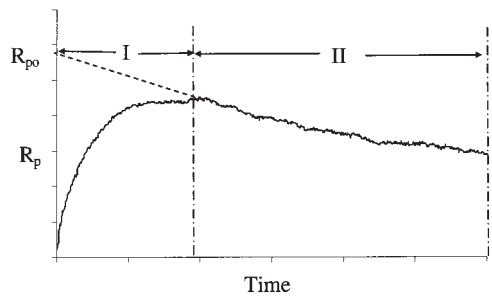

Figure 2. Kinetic curve obtained during propylene polymerization.

Table 2. Conditions and Results of Liquid-Pool Propylene Polymerization

Run No.	T °C	H_2 mg	$X \cdot 10^3$ [−]	Catalyst mg	$t_{reaction}$ min	Y gram	M_w^+ kg/mol	PDI	R_{po} kg/$g_{cat} \cdot$ hr	$R_{po,ATR}$ kg/$g_{cat} \cdot$ hr	k_d 1/hr	Y/A_1	Y/A_2
1	60	0	0	3.78	60	35.9	*3284*	—	8.5	11	0.288	1.91	1.93
2	60	150	1.33	3.78	60	132.9	266	6.5	54.7	62.7	0.900	2.21	2.12
3	60	1000	9.81	1.54	50	54	*106*	—	75.8	53.1	1.446	2.26	2.14
4	70	0	0	3.78	60	115	*3878*	—	16.1	9.6	0.342	1.92	1.86
5	70	25	0.24	3.78	60	163	1119	6.35	62.5	37.9	0.798	2.2	2.05
6	70	50	0.49	3.78	60	214	833	6.58	81.3	74.9	0.948	2.29	2.21
7	70	150	1.44	3.78	35	169.5	361	6.77	121.6	56.5	1.188	2.2	2.06
8	70	250	2.47	3.78	47	247.7	*294*	—	145.1	90.5	1.53	2.32	2.17
9	70	500	5.15	1.54	45	95.5	244	7.32	154.1	144.7	1.764	2.43	2.29
10	70	1000	9.94	1.54	45	90.3	*132*	—	139.6	89.9	1.932	2.05	1.92
11	75	150	1.56	3.78	35	232	—	—	208.5	120	2.26	2.01	1.95
12	80	0	0	3.78	60	81.5	*2818*	—	27.9	30.6	0.378	2.17	2.08
13	80	150	1.9	1.54	52	92	*393*	—	205.4	169.2	2.034	2.4	2.24
14	80	1000	12.4	1.54	32	92.3	143	5.7	252.4	130.4	3.21	2.48	2.3
15	70	150	1.50	3.78	7.5	47.8	NA	—	NA	NA	NA	2.95	1.95

Other polymerization conditions: 1040 mg TEA, 50 mg Donor.
Values in *italics* are calculated from intrinsic viscosity data.

Primary parameter estimation

The simplified model for constant monomer and hydrogen concentrations[2,3,37] is:

$$R_p = R_{po} \cdot \exp(-k_d \cdot t) \tag{3}$$

and can be used to fit a given isothermal polymerization rate profile with two parameters, R_{po} and k_d. The results of all 15 kinetic experiments are summarized in Table 2.

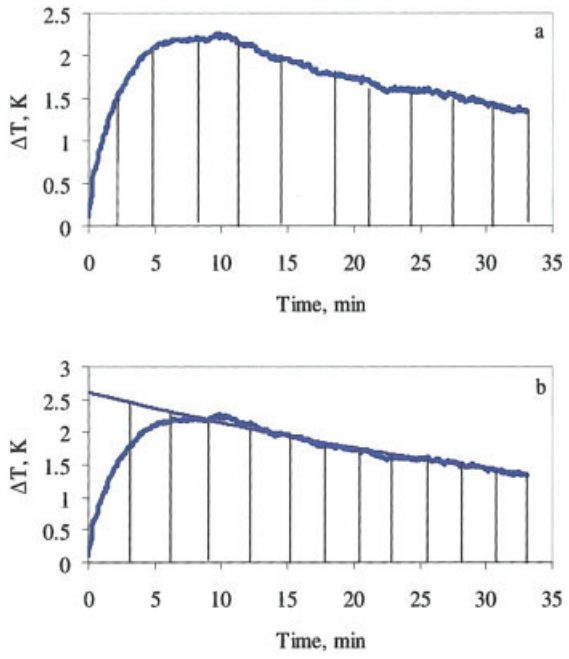

Figure 3. Area underneath the isoperibolic ΔT curve of run 7: (a) A_1; (b) A_2.

A_1 left, A_2 right hand side. [Color figure can be viewed in the online issue, which is available at www.interscience.wiley.com.]

Polymerization rate

Figure 5 shows the rate-time profiles for different temperatures and two hydrogen concentrations, namely, 0.0 mg (Runs 1, 4, and 12) and 150 mg (Runs 2, 7, and 13). It seems that the time between catalyst injection and reaching the maximum is quite uncertain at low polymerization rates (zero hydrogen), whereas at high polymerization rates this time interval slightly decreases with increasing temperature. Obviously, this is of minor importance for the kinetic interpretation: Y/A_2 has a value of approximately 2.0 for all experiments. Another effect seems to be more important: the higher the polymerization rate, the faster the catalyst decay, as will be seen in the sequel.

Figure 6 presents the Arrhenius plot of the initial polymerization rates R_{po} at different hydrogen concentrations. As expected, the polymerization rate decreases with decreasing temperature for different hydrogen concentrations, but two issues should be emphasized:

- The activation energy is virtually independent of the hydrogen concentration. The calculated activation energies are 58.6, 63.6, and 56.7 kJ/mol for 0.0, 150, and 1000 mg H_2, respectively, in the temperature range of 60-80°C. These values are consistent with the literature data.[2,8,38] The relative hydrogen response effect in terms of polymerization rate is the same for different temperatures.

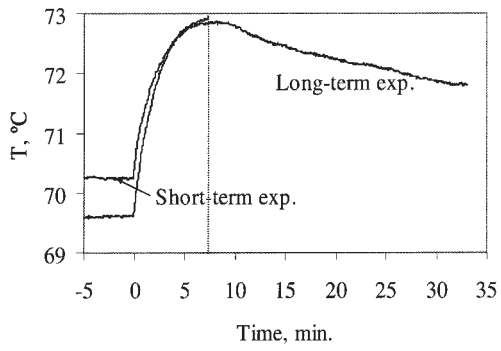

Figure 4. Temperature profiles for the long-term polymerization experiment and the short-term one.

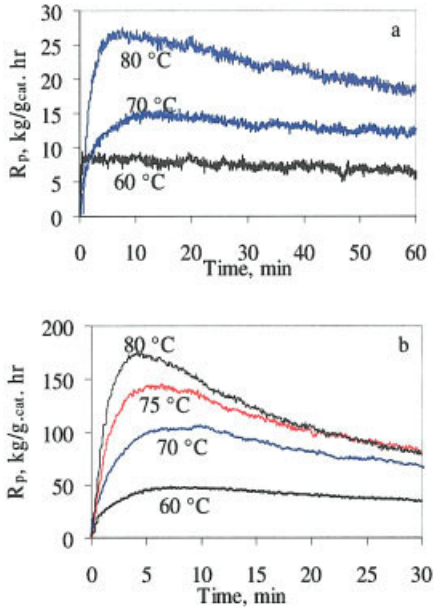

Figure 5. Polymerization rate-time profiles at different temperatures.

(a) 0.0 mg H_2 (Runs 1, 4, and 12), (b) 150 mg H_2 (Runs 2, 7, 11, and 13). [Color figure can be viewed in the online issue, which is available at www.interscience.wiley.com.]

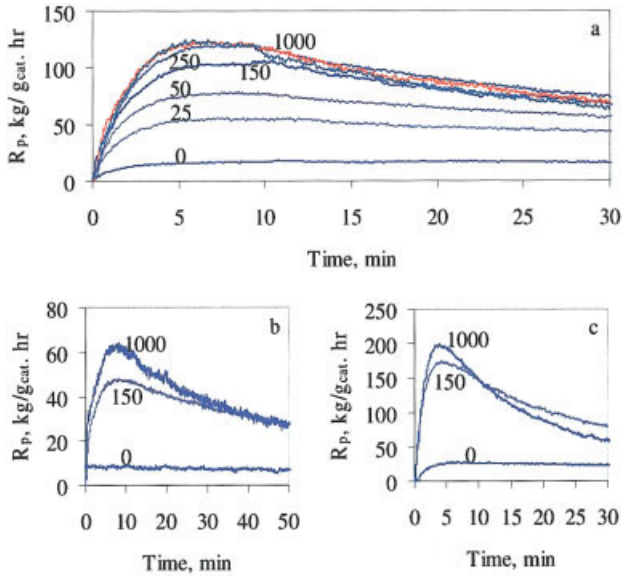

Figure 7. Polymerization rate-time profiles for different H_2 concentrations and temperatures.

(a) 70°C (Runs 4-10), (b) 60°C (Runs 1-3), (c) 80°C (Runs 13-15). [Color figure can be viewed in the online issue, which is available at www.interscience.wiley.com.]

• In the fully filled reactor, the initial polymerization rate does not flatten out or decrease with increasing temperature at relatively high temperatures. Note that this is not always the case for experiments in a partially filled reactor in the presence of a monomer gas phase operated under similar conditions (see [2,38]).

Figure 7 shows the rate profiles for different hydrogen concentrations at 60, 70, and 80°C. The presence of hydrogen in the reactor significantly increases the catalyst activity for all three temperatures studied.

In the absence of hydrogen, the catalyst shows low activity, which increases strongly with increasing hydrogen concentration at molar fractions, X, below 0.001, corresponding to 150 mg hydrogen injection in our experiments (see Table 2 and Figure 8); however, above this value, the impact of hydrogen levels off, and the initial reaction rate reaches a maximum value of about 75, 155, and 252 kg/g_{cat}.hr for 60, 70, and 80°C, respectively. Compared to the initial polymerization rates at zero hydrogen, this provides acceleration factors of 8.8, 9.7, and 9 for 60, 70, and 80°C, respectively—a constant, temperature independent value of about 9. This can be interpreted as follows:

For this catalyst, about 1/9 (11%) of the potentially active sites are really active if one assumes that all potentially active sites are active at the hydrogen plateau. This is in agreement with the kinetic data discussed by Rishina and coworkers.[9] This part is temperature independent, at least within the temperature and concentration ranges measured in this research. The activation energy of the initial polymerization rate is hydrogen independent; see Figure 8. Therefore, it can be assumed that the same ratio of potentially active sites is always blocked at zero hydrogen. Adding a given amount of hydrogen leads to similar acceleration effects at different temperatures, for example, at

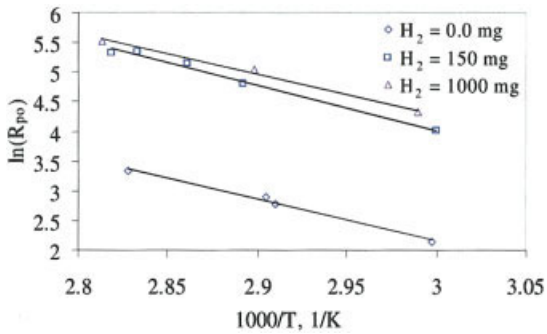

Figure 6. Arrhenius plot for the initial reaction rate at different H_2 concentrations.

[Color figure can be viewed in the online issue, which is available at www.interscience.wiley.com.]

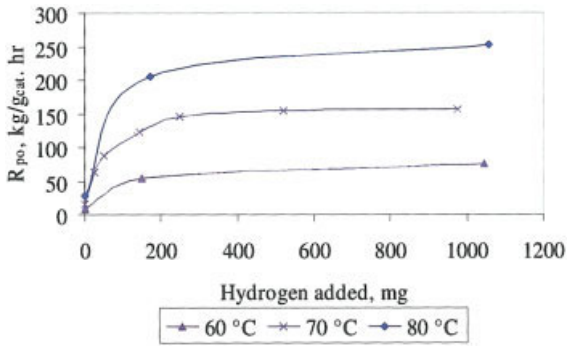

Figure 8. The effect of hydrogen on the initial reaction rate, R_{po}.

[Color figure can be viewed in the online issue, which is available at www.interscience.wiley.com.]

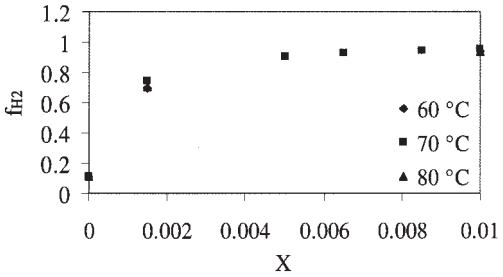

Figure 9. Hydrogen function for different temperatures.

150 mg hydrogen, the initial polymerization rates are 54.7, 121.6, and 205.4 kg/gcat hr for 60, 70, and 80°C, respectively. If one divides these values by the corresponding values at zero hydrogen, then one would get 6.4; 7.5, and 7.3 for 60, 70, and 80°C, respectively—again, a nearly constant (temperature independent) acceleration factor of about 7 under these conditions. Obviously, the curves shown in Figure 8 are shifted by adding hydrogen. Normalizing these curves leads to the "master" curve shown in Figure 9, which provides the evidence of the temperature independence of this shift effect that can be considered as a "kinetic fingerprint" for the given catalyst.

The plateau effect at high hydrogen concentrations has been confirmed by several authors.[2,4,9,14] Guastalla and Giannini[14] proposed the presence of adsorption phenomena of hydrogen on the surface of the solid catalyst, with a saturation at high concentrations. Rishina et al.[9] suggested that a limiting maximum number of active centers is realized in the catalytic system in the presence of hydrogen. This is in agreement with results presented by Samson et al.[4] and Pater et al.,[2] who assumed that the concentration of the blocked sites is very low at high hydrogen concentrations. Our results confirm these earlier results, now with more reliable data.

The deactivation constant increases with hydrogen concentration, as can be seen in Figure 10. The shape of the curves is quite similar to the shape of the R_{po} curves shown in Figure 8.

Figure 11 shows a linear relationship between R_{po} and k_d for all experiments: the more monomer converted by an active site, the higher the probability of deactivation, but independent of the reason for the higher polymerization rate. This way the deactivation can be interpreted as "activity-dependent probability." Additionally, one can conclude that an active site cannot deactivate during its dormant state. The low deactivation at zero hydrogen is caused by the high probability of being dormant, because of low reactivation rates by monomer transfer and propagation reactions. This supports the idea discussed previously by Pater et al.[2] and Roos et al.[39] that the deactivation of the catalyst relates to the catalyst activity independent of the reason for the activity change (temperature, pressure, hydrogen concentration, etc.). These experimental findings need to be interpreted.

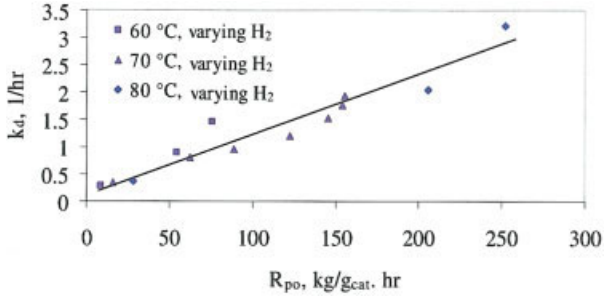

Figure 11. Deactivation constant versus initial polymerization rate, all runs, see Table 2.

[Color figure can be viewed in the online issue, which is available at www.interscience.wiley.com.]

Figure 12 shows the Arrhenius plot of the lumped first-order deactivation rate constant, k_d. The plot is linear for all hydrogen concentrations measured; again, there is no change of the slope at high temperatures. The results clearly indicate an increase in the activation energy with the increasing level of hydrogen at low hydrogen concentrations, but a constant value near 40 kJ/mol if more than 150 mg H_2 is used. Interestingly, at zero hydrogen, the activation energy is in the range of a diffusion (limited) process.[40,41] At zero hydrogen, the reactivation of dormant sites is realized via monomer transfer or propagation reactions. These reactions are very slow and show a low activation energy of 13.5 kJ/mol. The slope difference compared to high hydrogen concentrations is an indication that a second deactivation step dominates the temperature dependence of k_d shown in Figure 12. According to Guyot et al.,[32] the coordinated propylene monomer is either inserted into the growing polymer or decomposes into an inactive Π-allyl species and H atom that is added to the growing chain. The formation of Π-allyl species, according to the authors, accounts

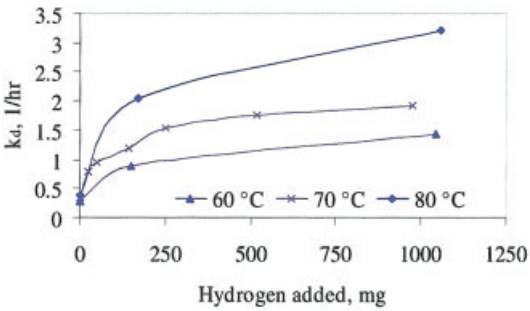

Figure 10. The influence of hydrogen on the deactivation constant.

[Color figure can be viewed in the online issue, which is available at www.interscience.wiley.com.]

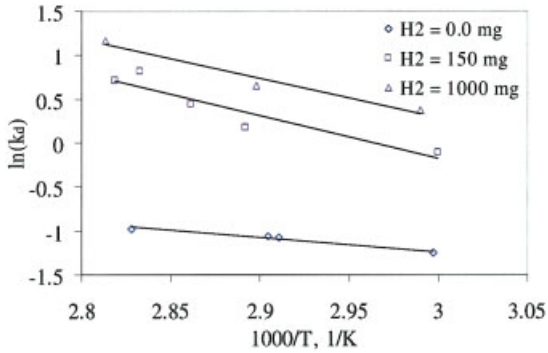

Figure 12. Arrhenius plot for deactivation constant at different H_2 concentrations.

[Color figure can be viewed in the online issue, which is available at www.interscience.wiley.com.]

for the high deactivation observed at high temperature. In terms of our results, this means: if Π-allyl species are responsible for the second deactivation step mentioned above, then both the higher deactivation and higher activation energy in the presence of hydrogen can be explained.

Molecular weight distribution

The effects of hydrogen concentration and temperature on molecular weight are summarized in Table 2. Similarly to other Ti-based polymerization catalysts,[8,21,22,24,42] the molecular weight decreases with increasing hydrogen concentration. Contrary to what is usually stated in different articles,[8,43,44] the molecular weight of the produced polymer increases with temperature. It is evident that the activation energy of the propagation reaction is higher than that of the transfer reaction under our conditions. Chadwick et al.[45] found that a 2,1-inserted center remains in the dormant state for a significant period of time even in the presence of hydrogen, and that the temperature increase can reduce the barrier to chain propagation after this misinsertion. This implies, according to the authors, that the molecular weight of the isotactic fraction may increase with increasing polymerization temperature, which is in agreement with what we found. The polydispersity trend indicates a slight narrowing of the MWD with increasing polymerization temperature, as can be seen in Table 2. This also indicates changing contributions of different active sites (different activation energies) with changing temperature; see [43,45,46].

Modeling

The modeling of reaction kinetics and molecular weight is based on the dormant site mechanism[47] using an "averaged-site" approach based on the following mechanism:

$$\text{Chain propagation} \quad C_j + M \xrightarrow{k_p} C_{j+1} \tag{4}$$

$$\text{Chain transfer to hydrogen} \quad C_j + H_2 \xrightarrow{k_h} C_o + D_j \tag{5}$$

$$\text{Chain transfer to monomer} \quad C_j + M \xrightarrow{k_m} C_1 + D_j \tag{6}$$

$$\text{Dormant site formation} \quad C_j + M \xrightarrow{k_s} S_{j+1} \tag{7}$$

$$\text{Dormant sites reactivation by } H_2 \quad S_j + H_2 \xrightarrow{k_{reh}} C_o + D_j \tag{8}$$

$$\text{Reactivation of dormant sites by monomer} \quad S_j + M \xrightarrow{k_{rem}} C_{j+1} \tag{9}$$

$$\text{Deactivation} \quad C_j \xrightarrow{k_d} D_j \tag{10}$$

Using the long chain hypothesis, the polymerization rate can be described as:

$$R_p = k_p \cdot C \cdot C_m \tag{11}$$

A sorption model should be used to describe the monomer concentration near the active sites, but a simplified model—using the concentration of liquid propylene directly—can be used.[34,48] The active catalyst site concentration, C, is the difference between the maximum concentration of active sites, C_{max}, and the concentration of dormant sites, C_S:

$$C = C_{max} - C_S \tag{12}$$

The concentration of dormant sites can be calculated assuming the quasi-steady-state:

$$R_S = 0 = k_S \cdot C \cdot C_m - k_{reh} \cdot C_S \cdot C_{H_2} - k_{rem} \cdot C_S \cdot C_m \tag{13}$$

Rearrangement of these equations results in:

$$C_S = \frac{k_S \cdot C}{k_{reh} \cdot X + k_{rem}} \tag{14}$$

where X is the hydrogen-monomer molar ratio:

$$X = \frac{C_{H_2}}{C_m} \tag{15}$$

Combining Eqs. 12 and 14 leads to:

$$C = \frac{C_{max} \cdot (1 + k_1 \cdot X)}{1 + k_2 + k_1 \cdot X} \tag{16}$$

with

$$k_1 = \frac{k_{reh}}{k_{rem}}; \quad k_2 = \frac{k_S}{k_{rem}} \tag{17}$$

This way the polymerization rate can be described as a function of three parameters, k_1, k_2, and k_p:

$$R_P = \frac{k_P \cdot C_m \cdot C_{max} \cdot (k_1 \cdot X + 1)}{1 + k_1 \cdot X + k_2} \tag{18}$$

or

$$R_p = k_p \cdot C_{max} \cdot C_m \cdot f_{H_2} \tag{19}$$

with the hydrogen dependent function f_{H_2} defined as:

$$f_{H_2} = \frac{1 + k_1 \cdot X}{1 + k_2 + k_1 \cdot X} \tag{20}$$

f_{H_2} represents the fraction of sites that are active under certain conditions, showing a minimum at X = 0 and a maximum, $f_{H_2,max} = 1$, at high values of X where all sites are activated.

The "quasi-single-site" approach results in an average termination probability:

$$q = \frac{2 \cdot M_M}{M_W} \tag{21}$$

For dormant sites of chain length j, $C_{S,j}$, it holds that

$$R_{S,j} = 0 = k_S \cdot C_{j-1} \cdot C_m - k_{reh} \cdot C_{S,j} \cdot C_{H_2} - k_{rem} \cdot C_{S,j} \cdot C_m \tag{22}$$

which gives:

$$C_{S,j} = \frac{k_S \cdot C_{j-1}}{k_{reh} \cdot X + k_{rem}} \tag{23}$$

The balance of the active sites of length j, C_j, can be written as:

$$R_{C,j} = 0 = -k_p \cdot C_j \cdot C_m + k_p \cdot C_{j-1} \cdot C_m - k_S \cdot C_j \cdot C_m + k_{rem} \cdot C_{S,j} \cdot C_m - k_h \cdot C_j \cdot C_{H_2} - k_m \cdot C_j \cdot C_m \tag{24}$$

Substituting $C_{S,j}$ in Eq. 23 into Eq. 24 gives:

$$C_j = p \cdot C_{j-1} \tag{25}$$

with the chain propagation probability, p:

$$p = \frac{1 + \frac{k_S/k_p}{X \cdot k_{reh}/k_{rem} + 1}}{1 + \frac{k_S}{k_p} + \frac{k_h}{k_p} \cdot X + \frac{k_m}{k_p}} \tag{26}$$

The termination (or chain transfer) probability q is defined by:

$$q = 1 - p = \frac{k_m}{k_p} + \frac{k_h}{k_p} \cdot X + \frac{k_s}{k_p} \cdot \left(\frac{k_1 \cdot X}{1 + k_1 \cdot X} \right) \tag{27}$$

with k_1 defined by Eq. 17.

One can model the weight average molecular weight M_w by combining Eqs. 21 and 27.

Parameter estimation

Equation 18 has three parameters to be determined, namely, k_p, k_1, and k_2. It should be emphasized that k_p is an average, because of the active sites heterogeneity; additionally, the true number of active sites and the true (in-situ) sorption is not taken into account and will influence the k_p value. For experiments without hydrogen, Runs 1, 4, and 12, Eq. 18 can be rewritten as:

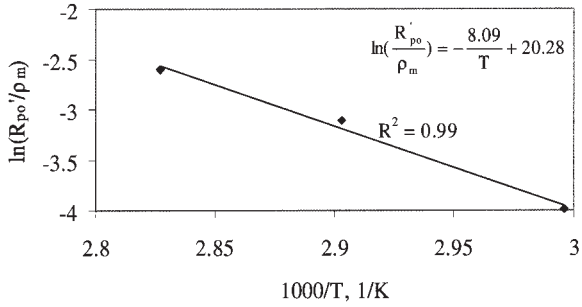

Figure 13. Calculation of propagation constant for propylene polymerization.

$$R'_{p,o} = \frac{k'_p}{1 + k_2} \cdot \rho_m \tag{28}$$

With known values for ρ_m (monomer density, kgm^{-3}), one can easily estimate the ratio $k_p/(1 + k_2)$, and a good Arrhenius fit (Figure 13) resulted with:

$$k_p = k_{po} \cdot (1 + k_2) \cdot \exp\left(-\frac{E_p}{R \cdot T} \right) \tag{29}$$

with

$$k_{po} = 6.41 \cdot 10^8 \ m^3/g_{cat} \cdot hr \tag{30}$$

$$E_p = 67.22 \cdot 10^3 \ J/mol \tag{31}$$

Nonlinear estimation of k_1 and k_2 gives the following results:

$$k_1 = -32.8 \cdot T^2 + 2.26 \cdot 10^4 \cdot T - 3.86 \cdot 10^6$$
$$k_2 = 8.02 \tag{32}$$

Figure 14 shows a comparison between the fitted model and the experimental data at 70 and 60°C.

Figure 11, as discussed earlier, shows an *almost* linear rela-

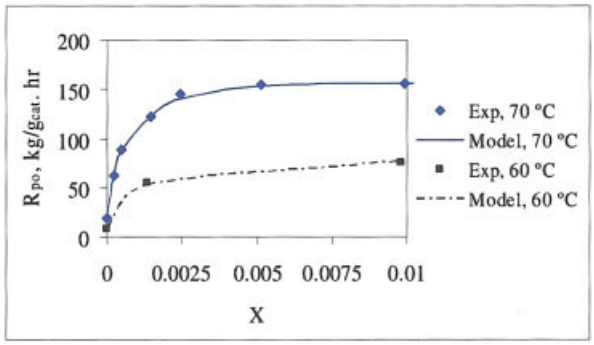

Figure 14. Comparison of model and experiment.

[Color figure can be viewed in the online issue, which is available at www.interscience.wiley.com.]

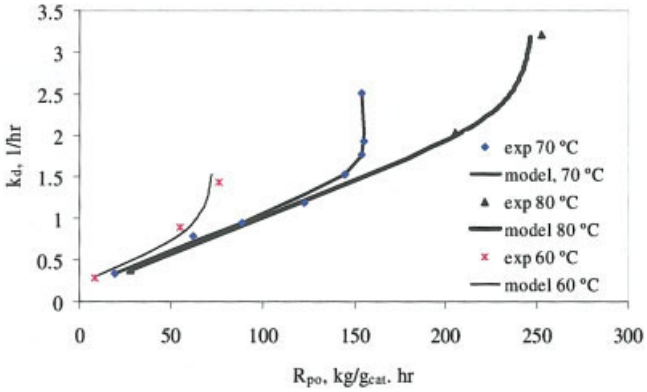

Figure 15. Comparison of model and experiment: k_d at 60, 70, and 80°C.

[Color figure can be viewed in the online issue, which is available at www.interscience.wiley.com.]

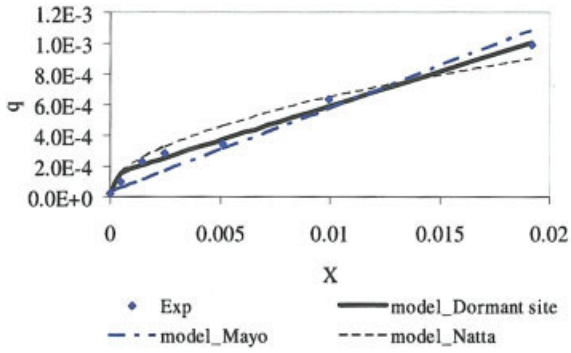

Figure 16. Test of different molecular weight models.

[Color figure can be viewed in the online issue, which is available at www.interscience.wiley.com.]

tionship between k_d and R_{po}. This suggests that the relationship between these variables can be described by a two-term function. The first term describes the linear behavior; meanwhile, the second term compensates for the deviation from the linearity. The following empirical relationship gives the best fit, as shown in Figure 15:

$$k_d = k_{d,1} \cdot R_{po} + k_{d,2} \cdot \exp\left[-\frac{E_{k_d}}{R \cdot T}\right] \cdot (1 + k_{d,3} \cdot X) \quad (33)$$

where

$$k_{d,1} = 8.38 \cdot 10^{-3}\ \mathrm{g_{cat}/kg} \quad (34)$$

$$k_{d,2} = 1.7 \cdot 10^{-4}\ \mathrm{1/hr} \quad (35)$$

$$k_{d,3} = 288.2 \quad (36)$$

$$E_{k_d} = -20 \cdot 10^3\ \mathrm{J/mol} \quad (37)$$

In Figure 15 the experimental data are compared to predictions using Eq. 33. As can be seen, the fit between model and experimental data is good at the three polymerization temperatures. Interestingly, this figure shows, also, that at low hydrogen concentration, <150 mg, the dependence of k_d on R_{po} can be described reasonably well using a linear relationship. However, increasing hydrogen concentration introduces deviations from linearity; where such a deviation becomes noticeable depends on the polymerization temperature. The physical reasoning for this deviation is still unclear. More research is required to interpret these findings.

According to the literature search above, one of the following models can be used to describe the average molecular weight:

(1) Square-root model, that is, Natta model;
(2) Linear model, that is, Mayo model;
(3) The dormant site model.[34,48]

The dormant site model gives the best fit; see Table 3 and Figure 16, with:

$$q = 2.077 \cdot 10^{-5} + 0.0448 \cdot X + 1.28 \cdot 10^{-4} \cdot \frac{15000 \cdot X}{1 + 15000 \cdot X} \quad (38)$$

Conclusions

Quasi-isothermal liquid propylene polymerization has been studied in a fully filled (over-pressured) batch reactor using a prepolymerized Ziegler-Natta catalyst with TEA as cocatalyst at different temperatures (60-80°C) and hydrogen concentrations (0-100 mmol/L). Polymerization rate profiles and molecular weight distributions have been measured and modeled with the following results:

(1) The adiabatic temperature rise in isoperibolic operation allows the estimation of initial polymerization rates after about 10 seconds. The catalyst used shows no significant activation after injection.

(2) Isoperibolic mode allows on-line estimations of the polymerization rate.

(3) The polymerization rate increases with increasing hydrogen, reaching a plateau at high hydrogen concentrations that

Table 3. Parameters of Different Average Molecular Weight Models

Model	A	B	C	D	R^2	SSE*
Linear model $q = A + B \cdot X$	$3.8 * 10^{-5}$	0.0545	—	—	0.94	$4.13 * 10^{-8}$
Natta model $q = A + B \cdot \sqrt{X/C_m}$	$2.0 * 10^{-5}$ $(\mathrm{mol/l})^{0.5}$	0.616	—	—	0.96	$2.73 * 10^{-8}$
This article $q = A + B \cdot X + C \cdot [D \cdot X/(1 + D \cdot X)]$	$2.077 * 10^{-5}$	0.0448	$1.28 * 10^{-4}$	15000	0.99	$8.02 * 10^{-9}$

*SSE: Sum of squares due to error.[50]

is about 9 times higher than polymerization rates at zero hydrogen. This effect does not depend on temperature.

(4) The pseudo-first-order deactivation constant is linearly dependent on initial polymerization rates.

(5) The rate of polymerization and the deactivation constant increase with temperature up to 80°C. The average activation energy of the polymerization rate is 58 kJ/mol, while the average activation energy of the deactivation process is considerably lower and is dependent on the hydrogen concentration.

(6) The polymer molecular weight decreases with hydrogen concentration, but increases with polymerization temperature.

(7) The polydispersity index increases slightly with the hydrogen concentration, but decreases with temperature.

(8) Both the polymerization rate and the molecular weight can be modeled using the dormant sites theory.

Acknowledgments

This work has been funded by Dutch Polymer Institute (DPI), project DPI #114. We greatly acknowledge R. Emonds and K. van Bree for the technical assistance. The authors further wish to thank Basell for the analytical support.

Notation

C = activated catalyst concentration, mol/L
C_{max} = concentration of active sites, mol/L
C_S = concentration of dormant sites, mol/L
C_m = concentration of monomer, mol/l
C_{H2} = hydrogen concentration, mol/l
C_j = growing polymer chain containing j monomers
E = activation energy, J/mol
D_j = dead (terminated) polymer chain containing j monomers
f_{H2} = fraction of potentially active sites
k_1 = k_{reh}/k_{rem}
k_2 = k_s/k_{rem}
k_d = deactivation rate constant, 1/h
k_h = chain transfer to hydrogen rate constant, l/mol. s
k_m = chain transfer to monomer rate constant, l/mol. s
k_p = propagation constant, l/mol. s
k_p' = propagation constant, m^3/g_{cat}. h
k_{reh} = dormant site reactivation by hydrogen rate constant, l/mol. s
k_{rem} = dormant site reactivation by monomer rate constant, l/mol. s
M_M = monomer molecular weight, g/mol
M_n = number average molecular weight, g/mol
M_v = viscosity average molecular weight, g/mol
M_w = weight average molecular weight, g/mol
p = propagation probability
q = termination probability
PDI = polydispersity index
R_p = polymerization rate, mol/l. s
R_p' = polymerization rate, kg/g_{cat} h
$R_{p,ATR}$ = polymerization rate based on adiabatic raise in temperature, kg/g_{cat}. h
T = polymerization temperature, °C
t = time, h
X = hydrogen molar ratio
Y = yield, gPP
ρ_m = monomer density, kg/m^3

Literature Cited

1. Pater JTM, Weickert G, van Swaaij WPM. Propene bulk polymerization kinetics: role of prepolymerization and hydrogen. *AIChE J.* 2003; 49:180-193.
2. Pater JTM, Weickert G, van Swaaij WPM. Polymerization of liquid propylene with a fourth generation Ziegler-Natta catalyst: influence of temperature, hydrogen, monomer concentration, and prepolymerization method on polymerization kinetics. *Chem Eng Sci.* 2002;57:3461-3477.
3. Shimizu F, Pater JTM, Van Swaaij WPM, Weickert G. Kinetic study of a highly active MgCl2-supported Ziegler-Natta catalyst in liquid pool propylene polymerization. II. The influence of alkyl aluminum and alkoxysilane on catalyst activation and deactivation. *J Applied Polym Sci.* 2002;83:2669-2679.
4. Samson JJC, Bosman PJ, Weickert G, Westerterp KR. Liquid-phase polymerization of propylene with a highly active Ziegler-Natta catalyst. Influence of hydrogen, cocatalyst, and electron donor on reaction kinetics. *J Polym Sci A: Polym Chem.* 1999;37:219-232.
5. Lim S, Choung S. Studies on the catalytic death in propylene polymerization. *Appl Catalysis A: General.* 1997;153:103-118.
6. Han-Adebekun GC, Hamba M, Ray WH. Kinetic study of gas phase olefin polymerization with a $TiCl_4/MgCl_2$ catalyst I. effect of polymerization conditions. *J Polym Sci A: Polym Chem.* 1997;35:2063-2074.
7. Forte MC, Coutinho FMB. The influence of catalyst system and polymerization conditions on polypropylene properties. *European Polym J.* 1996;32:605-611.
8. Soares JB, Hamielec A. kinetics of propylene polymerization with a non-supported heterogeneous Ziegler-Natta catalyst: effect of hydrogen on rate of polymerization, stereoregularity, and molecular weight distribution. *Polymer.* 1996;37:4607-4614.
9. Rishina LA, Vizen EI, Sosnovskaja LN, Dyachkovsky FS. Study of the effect of hydrogen in propylene polymerization with $MgCl_2$-supported Ziegler-Natta catalyst: Part 1. Kinetics of polymerization. *European Polym J.* 1994;30:1309-1313.
10. Chien J, Weber S, Hu Y. Magnesium chloride supported catalysts for olefin polymerization. XIX. Titanium oxidation states, catalyst deactivation, and active site structure. *J Polym Sci A: Polym Chem.* 1989; 27:1499-1514.
11. Chien J, Kuo C. Magnesium chloride supported high-mileage catalysts for olefin polymerization. X. Effect of hydrogen and catalytic site deactivation. *J Polym Sci A: Polym Chem.* 1986;24:2707-2727.
12. Chien J, Kuo C. Magnesium chloride supported high mileage catalyst for olefin polymerization. VII. Determination of concentration of titanium polymer and aluminum-polymer bonds. *J Polym Sci: Polym Chem Ed.* 1985;23:731-760.
13. Chien J, Kuo C. Magnesium chloride supported high mileage catalyst for olefin polymerization. VIII. Decay and transformation of active sites. *J Polym Sci Polym Chem.* 1985;23:761-786.
14. Guastalla G. Gianinni U. The influence of hydrogen on the polymerization of propylene and ethylene with an MgCl2 supported catalyst. *Macromol Chemie-Rapid Commun.* 1983;4:519-527.
15. Keii T, Suzuki E, Tamura M, Murata M, Doi Y. Propene polymerization with a magnesium chloride supported Ziegler catalyst: 1. Principal kinetics. *Macromol Chem Phys.* 1982;183:2285-2304.
16. Yuan HG, Taylor TW, Choi KY, Ray WH. Polymerization of olefins through heterogeneous catalysis. I. Low pressure propylene polymerization in slurry with Ziegler-Natta catalyst. *J Appl Polym Sci.* 1982; 27:1691-1706.
17. Naga N, Mizunuma K. Stereochemical control in propylene polymerization with non-bridged metallocene dichloride/MAO. *Polymer.* 1998;39:2703-2708.
18. Spaleck W, Kuber F, Bachmann B, Fritze C, Winter A. New bridged zirconocenes for olefin polymerization: binuclear and hybrid structures. *J Molecular Catalysis A: Chem.* 1998;128:279-287.
19. Al-haj Ali M, Betlem B, Roffel B, Weickert G. Propylene polymerization in a full-filled batch reactor. In preparation.
20. Natta G, Mazzanti G, Longi P, Bernardini F. Influenza dell'idrogeno sulla polimerizzazione anionica coordinata del propilene e dell' etilene. *La Chimica E L'Industria.* 1959;41:519-526.
21. Ross JF. Hydrogen as a chain terminator in continuous gas phase polymerization of propylene. *J Polym Sci A: Polym Chem.* 1984;22: 2255-2263.
22. Keii T, Doi Y, Suzuki E, Tamura M, Murata M, Soga K. Propene polymerization with a magnesium chloride-supported Ziegler catalyst, 2: Molecular weight distribution. *Macromol Chem Phys.* 1984;185: 1537-1557.
23. Soga K, Siono T. Effect of hydrogen on the molecular weight of polypropylene with Ziegler-Natta catalysts. *Polym Bull.* 1982;8: 261-268.
24. Kissin YV, Rishina LA, Vizen EI. Hydrogen effect in propylene

polymerization reactions with titanium-based Ziegler-Natta catalysts. II. Mechanism of the chain-transfer reaction. *J Polym Sci A: Polym Chem.* 2002;40:1899-1911.
25. Mori H, Endo M, Tashino K, Terano M. Study of activity enhancement by hydrogen in propylene polymerization using stopped-flow and conventional methods. *J Molecular Catalysis A-Chem.* 1999;145:153-158.
26. Busico V, Cipullo R, Corradini P. Ziegler-Natta oligomerization of 1-alkenes: a catalyst's "fingerprint", 1. *Macromol Chem Phys.* 1993; 194:1079-1093.
27. Kashiwa N, Yoshitake J. The influence of the valance state of titanium in MgCl2-supported titanium catalysts on olefin polymerization. *Makromolekulare Chemie.* 1984;185:1133-1138.
28. Busico V, Corradini P, Ferraro A, Proto A. Polymerization of propene in the presence of $MgCl_2$-supported Ziegler-Natta catalysts, 3: catalyst deactivation. *Makromolekulare Chemie.* 1986;187:1125-1130.
29. Albizzati E, Gianinni U, Collina G, Noristi L, Resconi L. Catalysts and polymerizations. In: Polypropylene Handbook. Moore E, ed. Munich: Carl Hanser Verlag; 1996:74-89.
30. Albizzati E, Giannini U, Balbontin G, Camurati I, Chadwick JC, Dall'occo T, Dubitsky Y, Galimberti M, Morini G, Maldotti A. Propylene polymerization with catalysts containing divalent titanium. *J Polym Sci A: Polym Chem.* 1997;35:2645-2652.
31. Chien J, Nozaki T. High activity magnesium chloride supported catalysts for olefin polymerization. XXIX. Molecular basis of hydrogen activation of magnesium chloride supported Ziegler-Natta catalysts. *J Polym Sci A: Polym Chem.* 1991;29:505-514.
32. Guyot A, Spitz R, Dassaud J, Gomez C. Mechanism of deactivation and reactivation of Ziegler-Natta catalysts for propene polymerization. *J Molecular Catalysis.* 1993;82:29-36.
33. Moritz HU. Polymerization calorimetry—a powerful tool for reactor control. In: *Polymer Reaction Engineering*. Berlin: VCH Weinheim; 1989:248-266.
34. Weickert G. High precision polymerization rate profiles. Presented at 3rd International Workshop on Heterogeneous Ziegler-Natta Catalysts, Kanazawa, Japan, 2003.
35. Tait PJT, Watkins ND. Monoalkene polymerization: mechanisms. In: *Comprehensive Polymer Science*. Oxford: Pergamon Press; 1989:533-573.
36. Keii T. *Kinetics of Ziegler-Natta Polymerization*. Tokyo: Kodansha LTD; 1972.
37. Samson JJC, Weickert G, Heerze A, Westerterp KR. Liquid-phase polymerization of propylene with a highly active catalyst. *AIChE J.* 1998;44:1424-1437.
38. Shimizu F. *Liquid Pool Polymerization of Propylene and Ethylene Using a Highly Active Ziegler-Natta Catalyst*, PhD Diss. Dept of Science and Technology. University of Twente, Enschede, The Netherlands, 2002..
39. Roos P, Meier GB, Samson JJC, Weickert G. Gas phase polymerization of ethylene with a silica-supported metallocene catalyst: influence of temperature on deactivation. *Macromol Chemie-Rapid Commun.* 1997;18:319-324.
40. Snijder ED, te Riele MJM, Versteeg GF, van Swaaij WPM. Diffusion coefficients of several aqueous alkanolamine solutions. *J Chem Eng Data.* 1993;38:475-480.
41. Scheible EG. Liquid diffusivities. *Industrial Eng Chem Research.* 1954;46:2007-2010.
42. Meier GB, Weickert G, Van Swaaij WPM. Gas-phase polymerization of propylene: reaction kinetics and molecular weight distribution. *J Polym Sci A: Polym Chem.* 2001;39:500-513.
43. Kissin YV, Ohnishi R, Konakazawa T. Propylene polymerization with titanium-based Ziegler-Natta catalysts: effects of temperature and modifiers on molecular weight, molecular weight distribution and stereospecificity. *Macromol Chem Phys*. 2004;205:284-301.
44. Yang CB, Hsu CC. Propene polymerization with $MgCl_2$-supported $TiCl_4$/dioctylphthalate catalyst. III. Effects of polymerization conditions on molecular weights and molecular weight distribution. *J Appl Polym Sci.* 1995;58:1245-1254.
45. Chadwick JC, Morini G, Balbontin G, Busico V, Talarico G, Sudmeijer O. Advances in propene polymerization using magnesium chloride-supported catalysts. *ACS Symposium Series 749: Olefin Polymerization Emerging Frontiers*. 2000;50-65.
46. Chien J. Olefin polymerizations and polyolefin molecular weight distribution. *J Polym Sci A: General Papers.* 1963;1:1839-1856.
47. Weickert G. *Modeling of Polymerization Rate and Molecular Weight: H_2 Response*. Internal report. Enschede, The Netherlands: IPP group, Twente University; 2002.
48. Banat Y, Veera UP, Weickert G. The role of equilibrium sorption in gas and liquid phase propylene polymerization. To be submitted to *Chem Eng Sci.*
49. Hindryckx F, Dubois P, Jérôme R, Marti MG. Ethylene polymerization by a high activity $MgCl_2$ supported Ti catalyst in the presence of hydrogen and/or 1-octene. *Polymer.* 1998;39:621-629.
50. Constantinides A, Mostoufi N. *Numerical Methods for Chemical Engineers with MATLAB Applications*. Upper Saddle River, NJ: Prentice Hall PTR; 1999.

Manuscript received July 6, 2005, and revision received Dec. 13, 2005.